Modeling and simulation of electrolyte pH change in conventional ISFET using commercial Silvaco TCAD

IOP Conf. Series: Materials Science and Engineering **518** (2019) 042020 doi:10.1088/1757-899X/518/4/042020

Modeling and simulation of electrolyte pH change in conventional ISFET using commercial Silvaco TCAD

Ahmed M. Dinar[1,2], AS Mohd Zain[1], F. Salehuddin[1], Mothana L. Attiah[1], M.K. Abdulhameed[1] and Mowafak k. Mohsen[1]

[1]Faculty of Electronics and Computer Engineering, Universiti Teknikal Malaysia Melaka (UTeM), Malacca, Malaysia;
[2]Computer Engineering, University of Technology, Baghdad, Iraq
E-mail: aealzubydi@gmail.com (Ahmed M. Dinar)

Abstract. This paper proposes a numerical simulation approach to study the electrolyte pH change of ion-sensitive field effect transistor (ISFET) structures using Silvaco technology computer-aided design (TCAD) tools. This paper examines the ISFET device's electrical response to electrolyte pH change. The modeling method is exploited by changing the potential surface charge depending on the electrolyte pH change and investigating how will it cause threshold voltage shift of ISFET device and other transfer characteristic parameters. The properties of a user-defined material offered by Silvaco are exploited to simulate the electrolyte behavior. The parameters of silicon semiconductor material (i.e., energy bandgap, permittivity, affinity, and density of states) are set to reconstruct an electrolyte solution. The electrostatic solution of the electrolyte area is investigated by giving a numerical solution for the semiconductor equation inside this area. Results show excellent agreement between theoretical model and self-consistency TCAD model. Additionally, transfer characteristics of a conventional ISFET device are simulated. The ID current as a function of the reference voltage VRef. and drain voltage VD for different pH scale and ID current as a function of VDS for different VRef. values for specific pH value are simulated. The proposed model allows accurate and efficient ISFET modeling by trying different designs and further optimization with commercial Silvaco TCAD tools rather than expensive fabrication.

Keywords: ion-sensitive field effect transistor (ISFET), electrolyte pH change, TCAD simulation, ISFET modeling

1. Introduction

The last decade witnessed a tremendous convergence in CMOS-based microtechnology, which plays a crucial role in chemical sensing applications. This was enabled using solid-state sensors that can be implemented in planar form and fabricated using CMOS technology that is monolithically integrated on a single chip. This now provides an opportunity for chemical sensing platforms to leverage semiconductor technology that may offer advantages such as scalability, miniaturization, fabrication, and integration with intelligent instrumentation. Ion-sensitive field effect transistor (ISFET) is the most promising sensor for satisfying all these opportunities [1]. ISFET is the chemical sensor that has many advantages, as follows:

high integration capability, low cost, simple interface, and high productivity. Furthermore, the most promising property is the scalability in developing semiconductor fabrication, especially in its CMOS technology implementation. This property provides many enhancements for biomedical sensors via sensor minimization, which increases the speed of the sensor and requires few solutions [2].

Surface charge density that makes the ISFET sensitive to pH is caused by chemical reactions between the ISFET gate dielectric on one side and the electrolyte on the other side [3][4]. In a conventional ISFET structure, the direct contact with solution is a sensing membrane called gate oxide. This area greatly influences the ISFET electrical behavior compared with the area of the entire sensor because of the existence of parasitic capacitance property, which degrades the ISFET sensitivity measurements. Protonation/Deprotonation reactions activate the surface charge potential (ψ_o) at the surface of ISFET. Coupling capacitance occurs between the surface and the float gate. This potential modulates the floating gate and shifts ISFET threshold voltage V_T [5][6]. The ISFET pH sensitivity is described and developed as a site-dissociation model by Yates [7].

Nevertheless, further research must examine more closely the links between IC design simulation and these models for more accurate analysis and further optimization; inopportunely, the famous commercial TCAD is not equipped with models, materials, and electrochemical processes that manage ISFET process and its operations [8]. Various approaches, such as experimental characterization, modeling[9] [10][3][11], and simulation, have been used on ISFET research work [12][13]. Until now, conventional ISFET has been modeled by different reports [14][15]. A part of conventional ISFET from these reports assumed that the energy band gap of electrolyte is zero voltage. The non-zero band gap model has many advantages, such as convergence problem compensation, especially with high states of density, and high agreement with roll-off sensitivity phenomena in conventional ISFET.

In this paper, we propose a numerical simulation approach to study the electrolyte pH change of conventional ISFET structures using Silvaco TCAD tools [16]. Furthermore, we examine the ISFET device electrical response (transfer characteristics) to electrolyte pH change. The remaining sections present the model description in three parts, as reported in Section 2. The model result, validation, and discussion of the ISFET and its transfer characterization are introduced in Section 3. The conclusions and future work are summarized in Section 4.

2. Model description

2.1 Surface potential model:

Surface charge density that makes the ISFET sensitive to pH is caused by chemical reactions between the ISFET gate dielectric on one side and the electrolyte on the other side [14], [15], [29], [38]–[40]. As a first step toward the development of a general methodology, we will chemically and mathematically improve this relationship. Chemically, when we choose the insulator material as a sensing membrane, ions will rest on the surface membrane of the insulator according to the pH concentration. Therefore, the surface potential (ψ_o) is calculated by the hydrogen ion H^+ exchange between electrolyte solution and site binding of an insulator. The pH sensitivity of good insulator should cover wide range of pH scale besides liner response to this range [17].

Mathematically, for an FET device:

$$V_G = V_{FB} + \frac{qN_A X_{d,T}}{C_{OX}} + \frac{qN_A (X_{d,T})^2}{2\varepsilon_s} \quad (1)$$

where V_G is the gate voltage, V_{FB} is flatband voltage, q is electronic charge, N_A is density of concentration, C_{OX} is the insulator capacitance per unit area calculated by $C_{OX}={}^{\varepsilon_{ox}}/_{t_{ox}}$, and $X_{d,T}$ is the depletion layer width that can be found by the following:

$$X_{d.T} = \sqrt{\frac{4\,\varepsilon_s\,\emptyset_F}{q\,N_a}} \tag{2}$$

where $\emptyset_F$= semiconductor work function = $\frac{K\,T}{q}\,\ln\frac{N_a}{n_i}$ (3)

Assume that: n_i= 1.43 e^{10} cm^{-3} for silicon,

and n_i= 1.92 e^{16} cm^{-3} for high-k material.

Therefore, $\emptyset_F$ = 4.17 eV for silicon and 4.59 eV for high-k material.

The previous equation shows that we can obtain different V_{FB} values for different V_G values. For ISFET device, we can rewrite Eq. (1) as follows [18]:

$$V_{th}^{T} = E_{ref.} - \psi_o + \chi^{sol} - \frac{Q_{Si}}{q} - \frac{Q_{ox}+Q_{SS}}{C_{ox}} \tag{4}$$

where E_{ref} , χ^{sol} , Q_{Si} , and Q_{ox} are reference electrode potential, electrolyte–insulator interface dipole, work function of silicon, and charge located in the oxide, respectively. Q_{SS} and C_{ox} are equivalent insulator–silicon interface charge and top-insulator capacitance per unit area, respectively. As mentioned in Section 1, the surface potential ψ_o modulates the floating gate and shifts ISFET threshold voltage V_T .Therefore, the Nernst equation control the proton activity at interface area that relates to potential is written as follows [19]:

$$\psi_o = \frac{kT}{q}\ln\frac{aH^{+}_{bulk}}{aH^{+}_{Surface}} \tag{5}$$

where *q* and *k* are elementary charge and Boltzmann constant, respectively. *a* is the proton activities in gate dielectric–electrolyte interface area and electrolyte. Therefore, we can conclude from (4) and (5) that the shift in threshold voltage for conventional ISFETs is given by the following:

$$V_{th}^{T} = -\Delta\psi_o \tag{6}$$

The site-dissociation model developed by Yates [7] describes the relationship between the change of potential with pH change, as follows:

$$\sigma_0(\psi_0) = qN_{sil}\left[\frac{cH_s^2 - K_aK_b}{cH_s^2 + K_b cH_s + K_aK_b}\right] \tag{7}$$

where $cH_s = cH_B exp\left(-\frac{q\psi_0}{kT}\right)$ (8)

where N_{sil} is the number of amphoteric silanol surface sites, and cH_S is the surface H^+ concentration. *Ka* and *Kb* are the surface dissociation constants.

2.2 Electrolyte pH change model

As mentioned in Section 1, the major challenge is the electrolyte simulation in commercial TCAD because it is not equipped with models, materials, and electrochemical processes that manage ISFET process and its operations [8]. Therefore, our idea exploits the user-defined material property offered by Silvaco to

simulate electrolyte solution [16]. The properties of a user-defined material offered by Silvaco are exploited to simulate the electrolyte (solution) behavior. The parameters of silicon semiconductor material (i.e., energy bandgap, permittivity, affinity, and density of states) are reconstructed in an electrolyte solution. Therefore, electrostatic solution of the electrolyte area can be investigated by giving a numerical solution for the semiconductor equation inside this area. Three types of materials are available in Silvaco Atlas, namely, semiconductor, insulator, and conductor. The procedure of defining a new material in Atlas (user-defined) specifies the material name, the user group it belongs to, and the last known atlas about the default material. When these parameters are set in their correct places in the Silvaco input deck code, we can change and manipulate the material properties using MATERIAL statements (i.e., permittivity, energy bandgap, affinity, and density of states) as is typically done [16].

The most important parameters that bind the electrolyte solution physical properties with the intrinsic semiconductor electrical parameters are density of states, conduction band NC, and valence band NV. These parameters play key roles in the molar concentration of the solution based on the following methodology. At the chemical equilibrium, the dissociation of H2O is (H+ + OH−). Thus, the mass action law at 25 °C and pure water is introduced by the following [20]:

$$K_{\omega} = [H^{+}]\,[OH^{-}] \tag{9}$$

$$H^{+} = OH^{-} = 1.0\; e^{-07} mol/L \tag{10}$$

Thus,
$$K_{\omega} = 1.0\; e^{-14} \tag{11}$$

The mass action law states that multiplying the free hole concentration p and the free electron n is equal to the square of the intrinsic carrier concentration n_i under thermal equilibrium. The carrier concentration can be given as follows, based on Boltzmann statistics [12]:

$$p = N_V\, e^{-\frac{E_f - E_v}{kT}} \tag{12}$$

$$n = N_C e^{-\frac{E_C - E_f}{kT}} \tag{13}$$

where E_V, E_C, and E_f are the upper energy level of the valence band, the lower value level of the conduction band, and the Fermi level, respectively.
If $p = [H^+]$, $n = [OH^-]$, and $n = p$ *from (10);* if $E_C - E_f = E_f - E_v = E_g/2$ from [21] Thus, we can rewrite (12) and (13) as follows:

$$N_C = ne^{\frac{E_g}{2kT}} \tag{14}$$

$$N_V = pe^{\frac{E_g}{2kT}} \tag{15}$$

Therefore, (14) and (15) clearly demonstrate the relationship between pH change in electrolyte and the density of state for valence and conduction band.

The site-binding model side can be updated based on the relation that described from (9) to (15) by replacing each H^+ with its semiconductor counterpart. The mass action law in (9) is the same as the relation $n_i^2 = np$. Therefore, we can rewrite (7) as follows:

$$\sigma_0 = qN_{sil}\left(\frac{p\, n_i^2 - K_a K_b n}{p\, n_i^2 + K_b\, n_i^2 + K_a K_b n}\right) \tag{16}$$

where the n_i is a constant, and only *p* and *n* will change with pH.

2.3 TCAD model

Commercial TCAD allows users to introduce bias-dependent surface charges in the form of interface donor or acceptor traps. The challenge is simulating the updated surface charge density equation described by (16) in the electrolyte pH change model [14]. To introduce this equation to the simulator, interface trap statements are utilized to mimic the surface charge accurately, as follows [16]:

"**INTTRAP** activates interface defect traps at discrete energy levels within the bandgap of the semiconductor and sets their parameter values. Device physics has established the existence of three different mechanisms, which add to the space charge term in Poisson's equation in addition to the ionized donor and acceptor impurities" [16]. Interface traps will add space charge directly into the right-hand side of Poisson's equation. To calculate the trapped charge in Poisson's equation, the total charge value is defined by the following:

INTTRAP <type> E. LEVEL= <r> DENSITY= <r> <capture parameters> (17)

where N_{tD}^{+} and N_{tA}^{-} are the densities of ionized donor-like and acceptor-like traps, respectively. DENSITY and its probability of ionization are represented as *FtA* and *FtD*, respectively. For donor-like and acceptor-like traps, the ionized densities are calculated by the following equations:

$$N_{tD}^{+} = \text{DENSITY} \times F_{tD} \tag{18}$$

$$N_{tA}^{-} = \text{DENSITY} \times F_{tA} \tag{19}$$

where *FtA* and *FtD* are given by the following equations:

$$F_{tA} = \frac{V_n\ SIGN\ n + e_{pA}}{V_n\ SIGN\ n + V_p\ SIGP\ p + e_{nA} + e_{pA}} \tag{20}$$

$$F_{tD} = \frac{V_p\ SIGP\ p + e_{nD}}{V_n\ SIGN\ n + V_p\ SIGP\ p + e_{nD} + e_{pD}} \tag{21}$$

where *SIGN* is the carrier capture cross sections for electrons and *SIGP* holes. The thermal velocities for electrons and holes are V_n and V_p , respectively. For donor-like traps, the electron and hole emission rates, e_{nD} and e_{pD}, are defined by the following [16]:

$$e_{nD} = \frac{1}{DEGEN.FAC}\ V_n\ SIGN\ n_i\ e^{E_t - E_i / kT} \tag{22}$$

$$e_{pD} = DEGEN.FAC\ V_p\ SIGP\ n_i\ e^{E_i - E_t / kT} \tag{23}$$

where *Et and Ei are* the trap energy level and the intrinsic Fermi level position, respectively. DEGEN.FAC is the degeneracy factor of the trap center. For acceptor traps, the electron and hole emission rates, e_{nA} and e_{pA} , are defined by the following [16]:

$$e_{nA} = DEGEN.FAC\ V_n\ SIGN\ n_i\ e^{E_t - E_i / kT} \tag{24}$$

$$e_{pA} = \frac{1}{DEGEN.FAC}\ V_p\ SIGP\ n_i\ e^{E_i - E_t / kT} \tag{25}$$

For example, the acceptor interface trap statement and its parameters are as follows:

Statement= INTTRAP **Type**= ACCEPTOR E.LEVEL = **value_1** DENSITY= **valu_2** INTMATERIAL= **"location of trap"** DEGEN. FAC = **value_3** EoN= **value_4** EoP=**value_5** SIGN= **value_6** SIGP=**value_7**

where seven parameters should be fitted to satisfy the TCAD interface trap system, as shown in the following table [22][15]:

Table 1. Interface Trap Parameters.

Value	Model
Value_1	$E_g/_2$
Value_2	N_{sil} based on insulator material type
Value_3	$DEGEN.FAC = \left(K_b \pm \sqrt{K_b^2 - 4K_aK_b}\right)/_{2n_i}$ for Donor-like
	$DEGEN.FAC = \frac{K_b n_i}{2K_aK_b}\left(K_b \pm \sqrt{K_b^2 - 4K_aK_b}\right)$ for Acceptor-like
Value_4	$EoN = DEGEN.FAC_{acceptor} K_aK_bn_i$ for Acceptor-like
	$EoN = 1/_{DEGEN.FAC_{donor}} K_aK_bn_i$ for Donor-like
Value_5	$EoP = 1/_{DEGEN.FAC_{acceptor}} n_i^3$ for Acceptor-like
	$EoP = DEGEN.FAC_{donor} n_i^3$ for Donor-like
Value_6	$\frac{K_aK_b}{V_n}$
Value_7	$\frac{n_i^2}{V_p}$

Considering all equations mentioned above, we can rewrite the sit-binding model (7) based on TCAD model. We first assume that acceptor and donor traps exchange carriers only with the conduction and valence band of the semiconductor representing the electrolyte, respectively. Hence, we can rewrite (7) in terms of TCAD model as follows:

$$\sigma_{(TCAD)} = q \times DENSITY\left(\frac{V_P\ SIGP\ P - V_n SIGN\ n}{v_P\ SIGP\ P + V_n SIGN\ n + K_b n_i^2}\right) \quad (26)$$

3. Results and discussion

3.1 Validation of models

An ISFET device is simulated to check the suitability of the modeling procedure. The cross-section of the ISFET simulation structure is shown in

Figure ***1***. The parameters required for validation and simulation are easily derived from the literature data (Table (2) to fit with experimental [3]) for SiO_2 gate dielectric to check the validity of our model and to show the agreement of models with the theoretical models and with experimental work. The first set of model validation examines the effect of changing pH on charge density in site-binding model. This is accomplished by comparing our models with the theoretical model developed by Yat [7] as shown in **Error! Reference source not found.**. Furthermore, the density of states *NC* and *NV* according to pH change values shown in Figure 3. We now turn to the experimental evidence on the comparison of the simulation of ISFET sensitivity with the standard real experimental that was done by ISFET developer Bergveld [3]. The results show good agreement between our model and the real experiment, as shown in Figure 4.

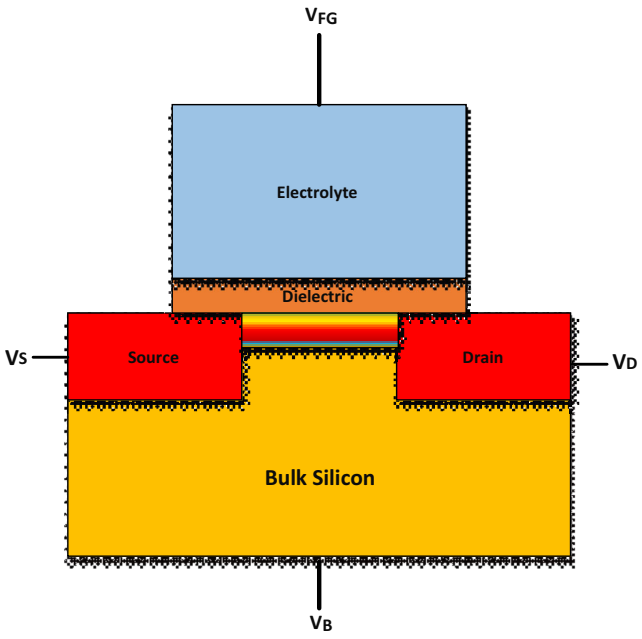

Figure 1. 2D Cross Section of ISFET

Parameter	Value	Unit	Parameter	Value	Unit
K_a	10^{-6}	-	Channel length	200	nm
K_b	10^{2}	-	S/D doping	10^{17}	cm^{-3}
N_{sil}	5.10^{14}	cm^{-2}	S/D length	50	nm
T	300	K	Electrolyte concentration	10^{-3}	Mol/L
k			Electrolyte permittivity	80	-
$t_{electrolyte}$	1000	nm	Oxide permittivity	3.9	-
t_{ox}	3	nm	V_{DS}	50	mV

Table 2. Simulation Parameters of ISFET in Figure 1.

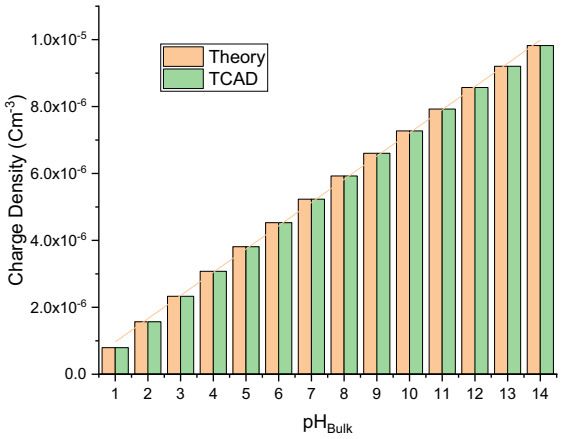

Figure 2. Comparison between the TCAD model and theoretical sit-binding model [7]

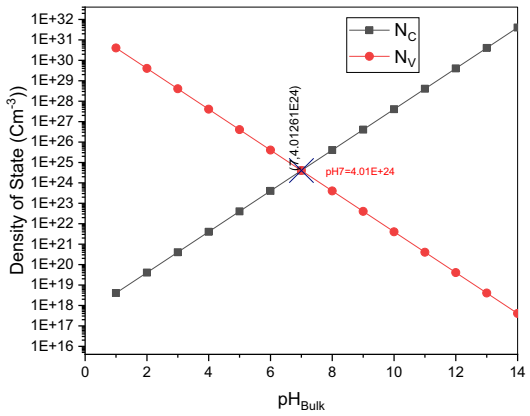

Figure 3. Variation of density of state of valence and conductance band according to pH change

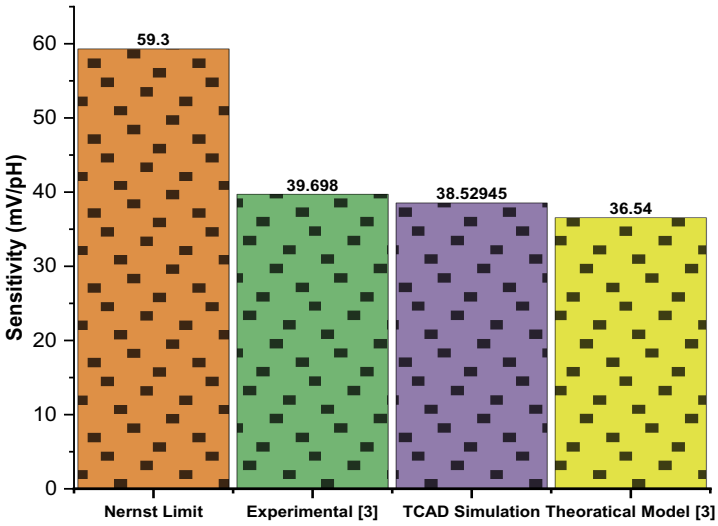

Figure 4: ISFET sensitivity validation

3.2. ISFET characterization

The electrostatic behavior (transfer characteristics) of a conventional ISFET device is simulated. Draining to source current I_{ds} versus the reference gate voltage $V_{Ref.}$ at various pH values for SiO_2 gate oxide layer is shown in **Error! Reference source not found.**. The observed increase in threshold voltage could be attributed to the increase in pH values. **Error! Reference source not found.** shows that the lowest and the highest values of pH report less sensitivity compared with values in the range pH 5–9, which is consistent with the theories [3].

Another transfer characteristic is draining source voltage V_{DS} for different pH scales in zero $V_{Ref.}$ and I_D current as a function of V_{DS} for different V_{GS} values for specific pH=7 value, as simulated and shown in **Error! Reference source not found.** and Figure *7*, respectively.

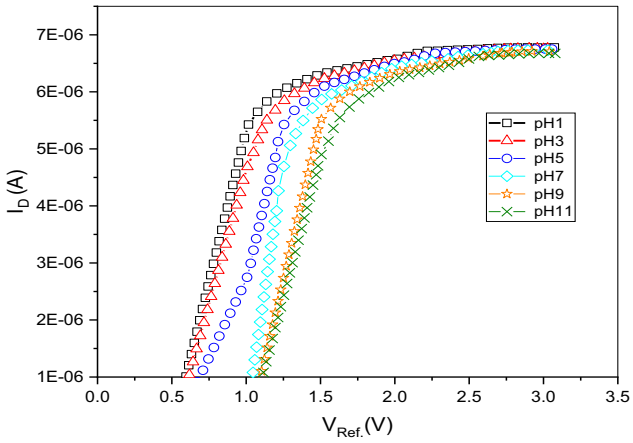

Figure 5. Transfer characteristics with respect to the reference gate voltage for SiO_2 gate oxide

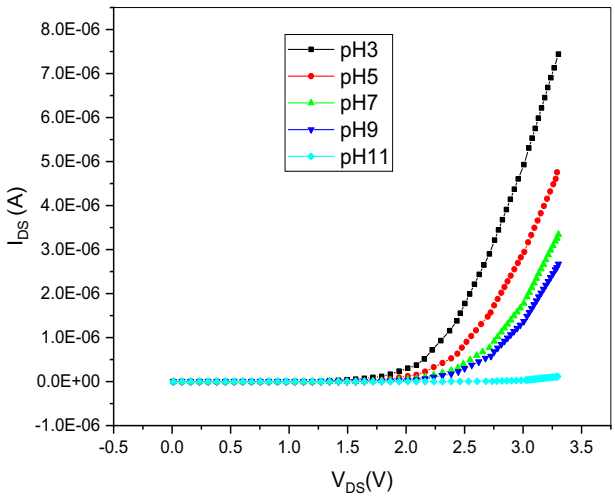

Figure 6. I_D vs. V_D for different pH solution with ($V_{Ref.}$ = 0).

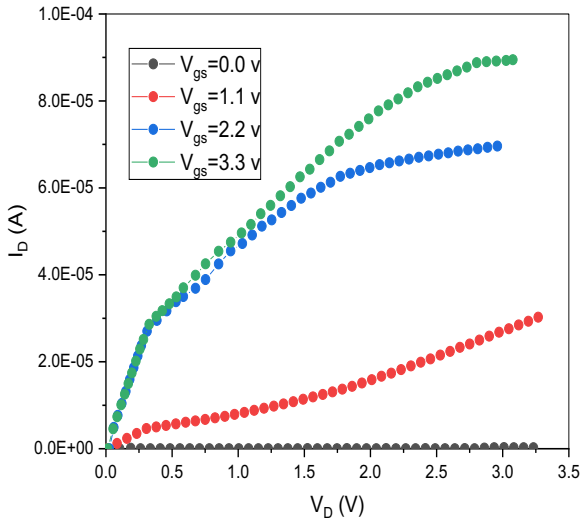

Figure 7. ID vs. V_D of the ISFET device for different $V_{Ref.}$ values.

4. Conclusion

A conventional ISFET, which uses simulation methods in addition to numerical modeling for pH sensing application, is proposed. The electrolyte pH change of ISFET device using Silvaco TCAD tools is investigated. The method exploits the properties of a user-defined material offered by Silvaco to simulate the electrolyte (solution) behavior. The parameters of silicon semiconductor material are set to reconstruct an electrolyte solution. Thus, the electrostatic solution of the electrolyte area can be investigated by giving a numerical solution for the semiconductor equation inside this area. The results show excellent agreement between theoretical model when comparing self-consistency TCAD model and real experimental work. Additionally, the transfer characteristics of a conventional ISFET device are simulated. The I_D current as a function of the $V_{Ref.}$ and V_{DS} for different pH scale and I_D current as a function of V_{DS} for different $V_{Ref.}$

values for specific pH value are simulated. The proposed model paves the way for accurate and efficient ISFET modeling by trying different designs and further optimization with commercial Silvaco TCAD tools rather than expensive fabrication. As a future work, we plan to make more transfer characteristics to verify our model with different real experimental research work for model expandability issue.

References

[1] Dinar A M, Zain A S M, and Salehuddin F 2018 UTILIZING OF CMOS ISFET SENSORS IN DNA APPLICATIONS DETECTION: A SYSTEMATIC REVIEW *Jour Adv Res. Dyn. Control Syst.* **10** 569–583.
[2] Dinar A M, Zain A S M and Salehuddin F 2017 CMOS ISFET device for DNA Sequencing : Device Compensation , Application Requirements and Recommendations *Int. J. Appl. Eng. Res.* **12** 11015–11028.
[3] Van H R E G, Eijkel J C T and Bergveld P 1996 A general model to describe the electrostatic potential at electrolyte oxide interfaces *Adv. Colloid Interface Sci.* **69** 31–62.
[4] Pan T M, Wang C W and Chen C Y 2017 Structural Properties and Sensing Performance of CeYxOy Sensing Films for Electrolyte–Insulator–Semiconductor pH Sensors *Sci. Rep.* **7** 2945.
[5] Chen B, Parashar A, and Pandey S 2011 Folded floating-gate CMOS biosensor for the detection of charged biochemical molecules *IEEE Sens. J.* **11** 2906–2910.
[6] Chi L L, Chou J C, Chung W Y, Sun T P and Hsiung S K 2000 Study on extended gate field effect transistor with tin oxide sensing membrane *Mater. Chem. Phys.* **63** 19–23.
[7] Healy W, Yates D E and Levine S Site-binding Model of the Electrical Double Layer at the Oxide / Water Interface *Trans. Farad. Soc.* **70** 1807, 1974.
[8] Tarasov A, *et al.* 2012 Understanding the electrolyte background for biochemical sensing with ion-sensitive field-effect transistors *ACS Nano* **6** 9291–9298,.
[9] Dinar A M, Zain A S M and Salehuddin F 2019 Comprehensive identification of sensitive and stable isfet sensing layer high-k gate based on isfet / electrolyte models **9** 926–933.
[10] Abdolkader T M 2013 A numerical simulation tool for nanoscale ion-sensitive field-effect transistor *Int. J. Numer. Model* **26** 493–505.
[11] Kaisti M, Zhang Q, Prabhu A, Lehmusvuori A, Rahman A and Levon K 2015 An Ion-Sensitive Floating Gate FET Model: Operating Principles and Electrofluidic Gating *IEEE Trans. Electron Devices* **62** 2628–2635.
[12] Passeri D, Morozzi A, Kanxheri K and Scorzoni A 2015 Numerical simulation of ISFET structures for biosensing devices with TCAD tools *Biomed. Eng. Online* **14** 1–16.
[13] Pittino F, Palestri P, Scarbolo P, Esseni D and Selmi L 2014 Models for the use of commercial TCAD in the analysis of silicon-based integrated biosensors *Solid. State. Electron.* **98** 63–69.
[14] Mohammadi E and Manavizadeh N 2017 Performance and sensitivity analysis of Dual-gated ion sensitive FET *25th Iran. Conf. Electr. Eng. ICEE 2017*, no. lCEE20 17, pp. 440–444.
[15] Bandiziol A, Palestri P, Pittino F, Esseni D and Selmi L 2015 A TCAD-based methodology to model the site-binding charge at ISFET/electrolyte interfaces *IEEE Trans. Electron Devices* **62** 3379–3386.
[16] Software D S 2016 ATLAS User ' s Manual," no. 408, pp. 567–1000.
[17] Spijkman M J, *et al.* 2010 Dual-gate organic field-effect transistors as potentiometrie sensors in aqueous solution *Adv. Funct. Mater.* **20** 898–905.
[18] Chou J C and Liao L P 2005 Study on pH at the point of zero charge of TiO2pH ion-sensitive field effect transistor made by the sputtering method *Thin Solid Films* **476** 157–161.
[19] Jang H J and Cho W J 2012 Fabrication of high-performance fully depleted silicon-on-insulator based dual-gate ion-sensitive field-effect transistor beyond the Nernstian limit *Appl. Phys. Lett.* **100**.

[20] Fromherz P, Offenhäusser A, Vetter T and Weis J 1991 A Neuron-Silicon Junction: A Retzius Cell of the Leech on an Insulated-Gate Field-Effect Transistor **252** 1290–1293.
[21] Pierret R F 1996 *Semiconductor Device Fundamentals* New York, p. 792.
[22] Mohammadi E and Manavizadeh N 2018 An Accurate TCAD-Based Model for ISFET Simulation *IEEE Trans. Electron Devices* **PP** 1–7.

.

Acknowledgment:
The authors would like to take this opportunity to highly appreciate the cooperation and the opportunity given by **Universiti Teknikal Malaysia Melaka (UTeM)** organization and **UTeM Zamalah Scheme** for funding this research.